

Electrostatic and Packing Contributions to the Structure of Water and Aqueous Electrolyte Solutions

M. F. Holovko, Yu. V. Kalyuzhny

Lviv Department of Statistical Physics, Institute for Theoretical Physics,
Ukrainian Academy of Sciences, Lviv, USSR

K. Heinzinger

Max-Planck-Institut für Chemie (Otto-Hahn-Institut), D-6500 Mainz, FRG

Z. Naturforsch. **45a**, 687–694 (1990); received January 31, 1990

The role of electrostatic and packing contributions to the structure of water and aqueous electrolyte solutions has been investigated by the comparison of results of Molecular Dynamics simulations with those of analytical calculations for the corresponding Lennard-Jones systems. It is demonstrated that the electrostatic interactions play a dominant role in determining the characteristic data of the various radial distribution functions in the solutions, although their relative importance decreases with increasing pressure, temperature, and ionic concentration. It is proposed that for the analytical treatment of hydrogen bonded liquids the total potential should be subdivided into three regions – short range repulsion, potential minimum, long range electrostatic interactions – and a different theoretical approach should be employed for each region.

1. Introduction

The application of statistical mechanics methods in liquid state theory (i.e. integral equations, cluster expansion, computer simulations) allows the prediction of properties of fluids and fluid mixtures starting from the intermolecular interactions. Considerable progress in the theory of unassociated liquids has been achieved along this line. It is based on the Lennard-Jones (LJ) type interparticle interaction. As for associated liquids and solutions the theory is more complicated and less developed. Usually a combination of LJ type (or similar ones) and electrostatic potentials is used to describe the interaction between the particles in this case. This type of the intermolecular potential provides the possibility to analyse the liquid structure in terms of packing and electrostatic contributions [1]. Here the former contribution is typical for unassociated liquids and depends mainly on the shape of the molecules [2–4], while in associated liquids the electrostatic interactions have a major effect on the structure as they introduce orientation dependent forces leading e.g. to the formation of hydrogen bonds. The relative role of these contributions to the structure of pure water has been investigated by extended Reference Interaction Site Model (RISM) calculations [5], and to the structure of pure methanol again by RISM

calculations [6] and Molecular Dynamics (MD) simulations [7].

This paper deals with the role of electrostatic and packing contributions to the radial distribution functions (RDF) of water and aqueous alkali halide solutions at various temperatures, pressures and concentrations. We shall compare the published RDFs from MD simulations [8–15] with new analytical calculations for the corresponding LJ liquids. In addition, this comparison provides the possibility to discuss the applicability of the LJ system as a reference one in the analytical description of water and electrolyte solutions [16]. A preliminary consideration of this problem was presented in [17].

2. Potentials and Calculations

In the MD simulations, the results of which are discussed here, the empirical rigid ST2 [18] and a flexible Central Force (CF) [19] model for water were employed. Both water models lead to very similar results as far as the RDFs are concerned, with the exception of the intramolecular peaks in $g_{OH}(r)$ and $g_{HH}(r)$, which have δ -like shape for the ST2 model and finite values for the CF model. We shall not make use of results with the flexible CF model, which allows the investigation of the effect of intermolecular interactions on the intramolecular geometry. In this paper we are concerned only with the intermolecular parts of

Reprint requests to Dr. K. Heinzinger, Max-Planck-Institut für Chemie, Saarstraße 23, D-6500 Mainz.

0932-0784 / 90 / 0500-0687 \$ 01.30/0. – Please order a reprint rather than making your own copy.



Dieses Werk wurde im Jahr 2013 vom Verlag Zeitschrift für Naturforschung in Zusammenarbeit mit der Max-Planck-Gesellschaft zur Förderung der Wissenschaften e.V. digitalisiert und unter folgender Lizenz veröffentlicht: Creative Commons Namensnennung-Keine Bearbeitung 3.0 Deutschland Lizenz.

Zum 01.01.2015 ist eine Anpassung der Lizenzbedingungen (Entfall der Creative Commons Lizenzbedingung „Keine Bearbeitung“) beabsichtigt, um eine Nachnutzung auch im Rahmen zukünftiger wissenschaftlicher Nutzungsformen zu ermöglichen.

This work has been digitalized and published in 2013 by Verlag Zeitschrift für Naturforschung in cooperation with the Max Planck Society for the Advancement of Science under a Creative Commons Attribution-NoDerivs 3.0 Germany License.

On 01.01.2015 it is planned to change the License Conditions (the removal of the Creative Commons License condition “no derivative works”). This is to allow reuse in the area of future scientific usage.

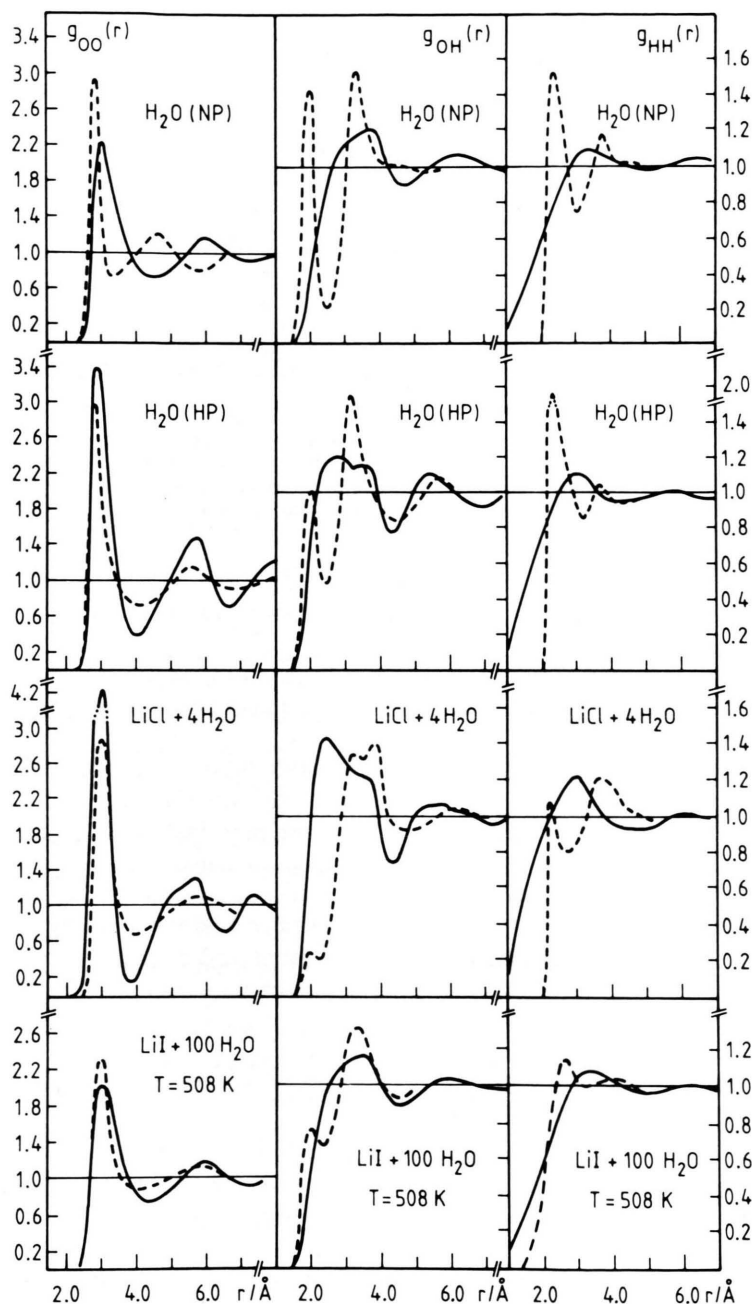


Fig. 1. Oxygen-oxygen, oxygen-hydrogen and hydrogen-hydrogen radial distribution functions from MD simulations (dashed) and from an analytical theory for the corresponding Lennard-Jones system (full) for pure water at temperatures of 336 and 350 K at densities of 0.9718 g/cm³ (first row) and 1.346 g/cm³ (second row), respectively, for water in a 13.9 molal LiCl solution (third row) and in a 0.55 molal LiI solution at 508 K (last row).

the RDFs. As they are almost the same for both water models we shall treat the results obtained with the CF model first as if they would have been derived from simulations with the ST2 model. The ion-water and ion-ion potentials employed, as well as further details of the simulations, are given in the original papers cited.

In the absence of electrostatic interactions the ion-molecular system reduces to the three component LJ mixture of atoms and molecules with auxiliary sites. The non-electrostatic contributions to the ion-ion, ion-oxygen and oxygen-oxygen RDFs coincide with the three kinds of pair distribution functions $g_{II}^{LJ}(r)$, $g_{IO}^{LJ}(r)$, and $g_{OO}^{LJ}(r)$ of the LJ mixture. The correspond-

ing oxygen-hydrogen, ion-hydrogen and hydrogen-hydrogen RDFs are expressed through $g_{\text{OO}}^{\text{LJ}}(r)$, $g_{\text{IO}}^{\text{LJ}}(r)$, and $g_{\text{OH}}^{\text{LJ}}(r)$, respectively, by simple relations [20]:

$$g_{\text{OH}}^{\text{LJ}}(r) = \frac{1}{2lr} \int_{|r-l|}^{r+l} g_{\text{OO}}^{\text{LJ}}(t) t \, dt,$$

$$g_{\text{IH}}^{\text{LJ}}(r) = \frac{1}{2lr} \int_{|r-l|}^{r+l} g_{\text{IO}}^{\text{LJ}}(t) t \, dt,$$

$$g_{\text{HH}}^{\text{LJ}}(r) = \frac{1}{2lr} \int_{|r-l|}^{r+l} g_{\text{OH}}^{\text{LJ}}(t) t \, dt,$$

where l is the intramolecular distance between oxygen and hydrogen. The calculations of $g_{\text{II}}^{\text{LJ}}(r)$, $g_{\text{IO}}^{\text{LJ}}(r)$ and $g_{\text{OO}}^{\text{LJ}}(r)$ have been performed within the scheme developed for the LJ systems by Weeks, Chandler, and Andersen [21].

3. Results and Discussion

In all the figures, the dashed curves show the results of simulations.

a) Water-Water RDFs

The RDFs for water as derived from the MD simulations are compared in Fig. 1 with those calculated from the analytical theory for the corresponding LJ system. From this comparison the relative role of electrostatic and packing contributions to the structure of water can be understood. In Fig. 1, results are presented for pure water with densities of 0.9718 and 1.346 g/cm³ and temperatures of 336 and 350 K, respectively, for water in a 13.9 molal LiCl solution and in a 0.55 molal LiI solution at 508 K. The high density in the case of pure water corresponds at the given temperature to a pressure of about 22 kbar.

It can be seen from the first row of Fig. 1 that for water at 1 bar and 336 K the additional electrostatic interactions result for $g_{\text{OO}}(r)$ in a shift of the first maximum to shorter distances, an increase of its height and a significant narrowing of the first peak which is responsible for the decrease of the number of nearest neighbors from the close packed case to about 5.5 [10]. All these changes are a consequence of hydrogen bond formation by the existence of polarity and with a preference for a tetrahedral arrangement of the nearest neighbor oxygen atoms. The second neighbor peak in the LJ system appears at a 1 Å larger distance than that of the MD simulation although both are of similar height. It is again a consequence of the stronger

interactions by the additional charges and is in agreement with the shortening of the first neighbor distance. The O–H and H–H RDFs change significantly more with polarity than $g_{\text{OO}}(r)$ as they are mainly determined by the relative orientation of the neighboring water molecules in the liquid which is, of course, very sensitive to changes in hydrogen bonding. Therefore, the two rather well defined peaks in $g_{\text{OH}}(r)$ and $g_{\text{HH}}(r)$ from the MD simulation are replaced in both cases by one broad maximum for the LJ system. It extends in the O–H RDF from $\sigma + r_{\text{OH}}$ to $\sigma - r_{\text{OH}}$, where r_{OH} denotes the intramolecular O–H distance of about 1 Å, and where $\sigma = 3.1$ Å is that of the ST2 model for water. In the H–H RDF the maximum for the LJ system appears between the two MD peaks at about 3.2 Å. These results are very similar to those obtained by Rossky from extended RISM calculations [22].

At a pressure of 22 kbar a partial break down of the hydrogen bond network occurs [10, 23]. It can be seen from the second row of Fig. 1 that the first peaks in the two $g_{\text{OO}}(r)$ almost coincide and consequently the second peaks appear at the same distance. The higher maxima in the case of the LJ system indicate enhanced structure when there is no electrostatic interaction. As from the three water-water RDFs $g_{\text{OO}}(r)$ is least sensitive to hydrogen bonding, the change in the packing contribution by the increased density overcompensates here the electrostatic contribution. The results of the MD simulation show that the partial break down of the hydrogen bond structure causes only a change of the relative heights of the peaks in $g_{\text{OH}}(r)$ and $g_{\text{HH}}(r)$ without a change in their positions. It is, at the other side, inherent to the LJ system that the increase in density can hardly change the O–H and H–H RDFs. Therefore, the increased density does not lead to a significant change in the relative roles of the electrostatic and packing contributions to $g_{\text{OH}}(r)$ and $g_{\text{HH}}(r)$.

The disturbance of the hydrogen bond structure of water by the introduction of ions depends strongly on the kind of ions and their concentration. The results obtained from MD simulations indicate that this disturbance is rather small in alkali halide solutions up to concentrations of 2.2 molal [14]. Therefore, a discussion of such solutions seems not to be warranted here. The situation changes significantly at higher concentrations. In the third row of Fig. 1 the results for a 13.9 molal LiCl solution are presented [11]. The effect of the ions on the relative role of electrostatic and packing contributions to the structure of water is at

this concentration even more important than the pressure increase by 22 kbar. The positions of the first two maxima and of the first minimum in $g_{OO}(r)$ coincide. It can be deduced from the differences in the heights that the electrostatic interactions have a negative influence on the short and long range structure of the corresponding LJ system. The splitting of the broad maximum in $g_{OH}(r)$, which was indicated already in the high pressure case, becomes more pronounced. A new maximum at shorter distances develops in this way, which almost coincides with that from the MD simulation. But the height of the latter one has become very small because of the almost complete break down of the hydrogen bond network. The orientation of the water molecules is at this concentration almost solely determined by the ion-water interactions. It is still not arbitrary and can, therefore, not be described correctly by the LJ system. This conclusion is supported also by the comparison of the two H–H RDFs.

In the last row of Fig. 1 the effect of temperature on the electrostatic and packing contributions to the structure of water is demonstrated. Presented are results for a 0.55 molal LiI solution at 508 K [13]. The effect of the ions can be neglected at this concentration. Although the pressure corresponds to 3 kbar at this temperature, still almost all of the changes have to be attributed to the change in temperature. It is obvious from the figure that the increase in temperature reduces the contribution of the electrostatic interaction on the structure of water much more than an increase in ionic concentration or pressure. MC studies of TIPS2 water at 773 K and 30 kbar and the corresponding LJ system by Kalinichev confirm this conclusion [24].

b) Ion-Water RDFs

In Fig. 2 the results of the investigation of the importance of electrostatic interactions for the ion-water RDFs are presented for a 2.2 molal NaCl solution under normal temperature and pressure, for the same solution at a pressure of 10 kbar, for a 0.55 molal LiI solution at 508 K and – for comparison – for a solution of argon in water. As before, the results of the MD simulations or – in the case of argon – the MC calculations are compared with those from an analytical theory for the corresponding LJ system. The electrostatic contributions to the structure of the hydration shells of the ions are significantly larger than those to the structure of water. The ion-oxygen and ion-hydrogen RDFs show similar features as the O–O

and O–H ones, respectively. This is a consequence of the orientation of the water molecules in the hydration shells of the ions, where the dipole moment of the water molecule points preferentially away from the cation while the anion forms preferentially linear hydrogen bonds with its nearest neighbor water molecules.

In the last row of Fig. 2 the argon-oxygen and argon-hydrogen RDFs from an MC simulation [25] are compared again with results from an analytical treatment of the corresponding LJ system. As expected there is excellent agreement as far as $g_{ArO}(r)$ is concerned. The differences in $g_{ArH}(r)$ are similar to those of $g_{OH}(r)$ as discussed above. They result from the fact that the hydrogen bonding of water leads also to a preference for certain Ar–H distances while the LJ system necessarily leads to a uniform distribution of the O–Ar–H angle resulting in a broad peak in the range 2–4 Å.

It can be seen from the first row in Fig. 2 that the electrostatic contributions to $g_{ClO}(r)$ and $g_{NaO}(r)$ are qualitatively similar but – because of the ions involved – necessarily stronger than in the case of $g_{OO}(r)$. The differences between the MD data [10] and the LJ system in the positions of the first and second maxima as well as in the heights strongly depend upon the size of the ion. The broad maxima in $g_{ClH}(r)$ and $g_{NaH}(r)$ for the LJ system are quite similar to that in $g_{OH}(r)$, and their positions shift necessarily with the maxima in the ion-oxygen RDFs. The effect of the electrostatic contribution to $g_{ClH}(r)$ is very similar to that for $g_{OH}(r)$ because of the preferentially linear hydrogen bond formation between the anion and its nearest neighbor water molecules. The strong interactions between Na^+ and the water molecules in its first hydration shell prevent hydrogen atoms to appear between Na^+ and O and, therefore, the electrostatic interactions do not cause a shift of the position of the broad peak in $g_{NaH}(r)$, but make it only significantly sharper. Otherwise the same arguments as discussed above in connection with $g_{OH}(r)$ hold for $g_{ClH}(r)$ and $g_{NaH}(r)$.

The changes in the relative contribution from electrostatic and LJ interactions with pressure in the Cl–H and Na–H RDFs are again similar to the ones in $g_{OH}(r)$ and need, therefore, no further discussion. The same holds for $g_{ClO}(r)$ in respect to $g_{OO}(r)$ with the exception that the two peaks remain separated. Only the Na–O RDF shows some qualitatively different features with pressure increase than the $g_{ClO}(r)$ and $g_{OO}(r)$ do. The pressure increase is not sufficient to

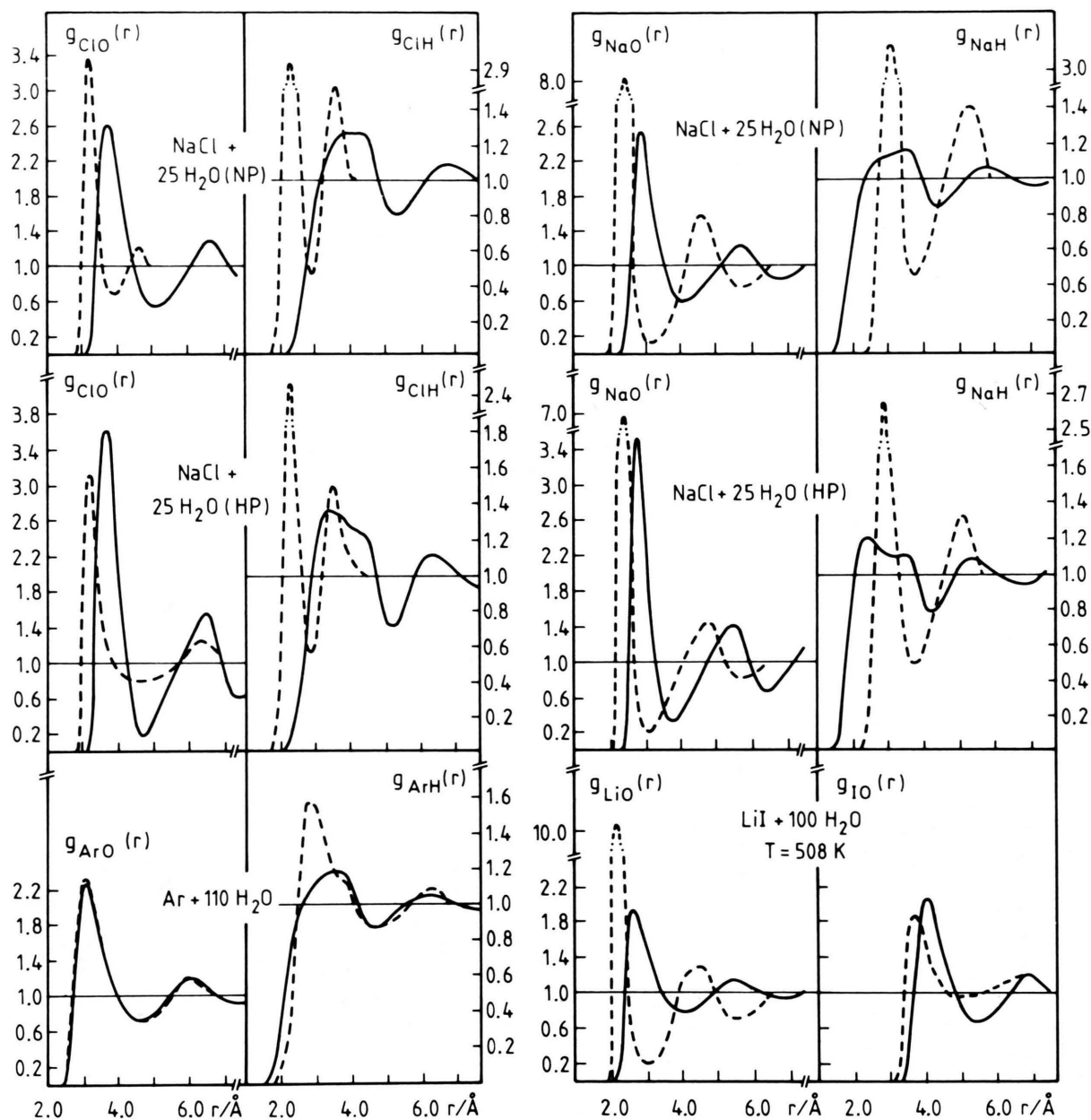


Fig. 2. Ion-oxygen, ion-hydrogen as well as argon-oxygen and argon-hydrogen radial distribution functions from MD simulations (dashed) and from an analytical theory for the corresponding Lennard-Jones system (full) for a 2.2 molal NaCl solution at room temperature and pressures of 1 bar and 10 kbar and for a 0.55 molal LiI solution at 508 K.

compensate the electrostatic effect. Therefore, the positions of the first and second maxima do not coincide, only the heights of the second peaks are nearly the same. Obviously, with the short Na–O first neighbor distance a limit is reached beyond which the electrostatic interactions cannot be compensated by pressure.

Finally, in the third row of Fig. 2 the effect of temperature on the relative role of electrostatic and LJ contributions to the Li–O and I–O RDFs is demonstrated. The MD curves result again from the simulation of a 0.55 molal LiI solution at 508 K [13]. Different from the $g_{\text{OO}}(r)$ case, where this temperature

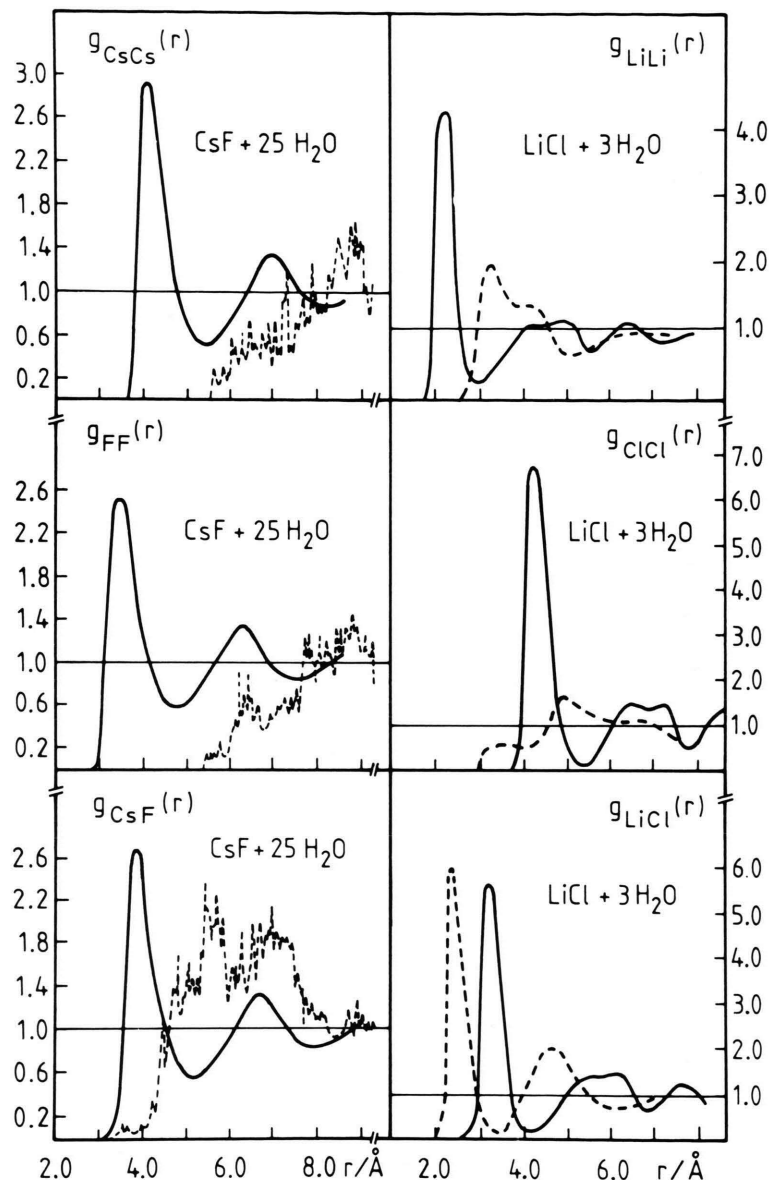


Fig. 3. Ion-ion radial distribution functions from an MD simulation (dashed) and from an analytical theory for the corresponding Lennard-Jones system (full) for a 2.2 molal CsF and a 18.5 molal LiCl solution.

increase almost completely compensates the electrostatic contributions as discussed above, in the Li–O and I–O RDFs the difference in the positions of the maxima remains. In analogy to $g_{\text{ClO}}(r)$ and $g_{\text{NaO}}(r)$, the electrostatic contributions at 508 K cause a slight decrease of the first maximum in $g_{\text{IO}}(r)$ and a significant increase in $g_{\text{LiO}}(r)$. As in the high pressure case, the electrostatic interactions between a sufficiently small ion and its first neighbor water molecules cannot be compensated at 508 K.

c) Ion-Ion RDFs

The electrostatic and packing contributions to the ion-ion RDFs are demonstrated in Figure 3. The results for a 2.2 molal CsF solution [26] and a 18.5 molal LiCl solution [15] are depicted as examples. The RDFs from the MD simulations are again compared with those from analytical calculations for the corresponding LJ system. The relatively small number of ions in the CsF solution leads to a strong noise in the

ion-ion RDFs derived from the MD simulation, but still the essential features of the electrostatic contributions can be seen.

The σ -values in the LJ potential describing the Cs^+-Cs^+ and F^--F^- interactions differ only slightly. Therefore, the positions and the heights of the maxima in the ion-ion RDFs for the 2.2 molal CsF solution are quite similar for the LJ system. It can be seen from Fig. 3 that for the like ions the Coulombic repulsion prevents the formation of a nearest neighbor shell. The broad maxima in $g_{\text{CsCs}}(r)$ and $g_{\text{FF}}(r)$ indicated at about 8–9 Å roughly coincide with the position of the minimum in $g_{\text{CsF}}(r)$. This means that the electrostatic interactions lead to an order where a central ion is surrounded by water molecules followed by counterions, and after a second water layer again an ion follows with the same charge as the central one. In agreement with this order, the broad peak centered around 6 Å in the RDF for the unlike ions results from a cesium ion separated by a water molecule from a fluoride ion. There is an indication of a peak at about 3.5 Å in $g_{\text{CsF}}(r)$ which could mean the existence of a contact ion pair. The running integration would indicate that one out of ten ions forms a contact ion pair [26]. Its position is at a shorter distance than that of the first peak in the LJ system because of the Coulombic attraction.

In the 18.5 molal LiCl solution the different sizes of the ions lead to significant differences in the positions of the maxima and their heights in the ion-ion RDFs of the LJ system. The generally higher first peaks when compared with those in the CsF solution are a consequence of the higher concentration. The broad and splitted second peaks result again from the differences in the ion size. The Coulombic repulsion between the like ions cannot lead to an order as discussed above for the less concentrated CsF solution because of the lack of a sufficient number of water molecules. Therefore, the first maximum in $g_{\text{LiLi}}(r)$ has been interpreted as resulting from two Li^+ separated by one water molecule in the appropriate geometry while the pronounced shoulder at about 4 Å could result from two Li^+ in contact with the same Cl^- [15]. The electrostatic interactions strongly broaden the first peak in $g_{\text{ClCl}}(r)$, which extends now from 3 Å – the distance of a contact Cl^- pair – up to 7 Å without a strong deviation from the uniform density in the whole distance range. It seems that at this high ionic concentration the repulsive negative charges of two Cl^- can be overcome by their interaction with the same Li^+ . It is

obvious from the position of the first peak in the Li–Cl RDF that contact ion pairs are formed. The second peak simply reflects the distances expected for a water molecule separated ion pair.

5. Conclusions

The comparison of the various RDFs in aqueous electrolyte solutions as derived from MD simulations with those from analytical calculations for the corresponding LJ systems reveals the major role of electrostatic interactions for the description of the water structure, the structure of the hydration shells of the ions, and the ionic order in the solutions. This conclusion remains valid although it can be seen that the importance of the electrostatic contributions to the water–water, ion–water, and ion–ion RDFs decreases with increasing temperature, pressure, and ionic concentration in favor of the packing contributions.

It follows from this investigation that the pure LJ system is a rather poor choice as reference system in the analytical treatment of water and aqueous electrolyte solutions. The depth and the position of the potential minimum strongly depend upon the electrostatic interaction. It has been found from various MD simulations that the position of the first maxima in the ion–oxygen and oxygen–oxygen RDFs almost coincide with the position of the global minima of the corresponding pair potentials [9]. Therefore, it is obvious that the Coulombic interactions at short distances have to be included into the reference system in order to describe reliably the important features of the RDFs. It can be concluded from this investigation that the analytical approach for hydrogen bonded liquids must be based on the presentation of the total potential as a sum of three terms which cover separately the short range repulsion, the region of the global potential minimum, and the long range electrostatic interactions. Each of the three terms has to be treated by a different theoretical approach.

Acknowledgements

The authors thank Professor I. R. Yukhnovsky and Dr. G. Pálinkás for helpful discussions. Financial support by the Ukrainian Academy of Sciences and Deutsche Forschungsgemeinschaft is gratefully acknowledged.

- [1] P. J. Rossky, *Ann. Rev. Phys. Chem.* **36**, 321 (1985).
- [2] J. A. Barker and D. Henderson, *Rev. Mod. Phys.* **48**, 487 (1976).
- [3] I. R. Yukhnovsky and M. F. Holovko, *Statistical Theory of Classical Equilibrium Systems*. Naukova Dumka, Kiev 1980.
- [4] D. Chandler, in: *The Liquid State of Matter: Fluids Simple and Complex* (E. W. Montroll and J. L. Lebowitz, eds.), North-Holland, Amsterdam 1982.
- [5] B. M. Pettit and P. J. Rossky, *J. Chem. Phys.* **77**, 1451 (1982).
- [6] B. M. Pettit and P. J. Rossky, *J. Chem. Phys.* **78**, 7296 (1983).
- [7] G. Pálkás, Y. Tamura, E. Spohr, and K. Heinzinger, *Z. Naturforsch.* **43a**, 43 (1988).
- [8] K. Heinzinger and G. Pálkás, in: *The Chemical Physics of Solvation, Part A* (R. R. Dogonadze, E. Kálman, A. A. Kornyshev, and J. Ulstrup, eds.), Elsevier, Amsterdam 1985.
- [9] K. Heinzinger, *Physica* **131B**, 196 (1985).
- [10] G. Jancsó, P. Bopp, and K. Heinzinger, *Chem. Phys.* **85**, 377 (1984).
- [11] P. Bopp, I. Okada, H. Ohtaki, and K. Heinzinger, *Z. Naturforsch.* **40a**, 116 (1985).
- [12] G. Jancsó, K. Heinzinger, and P. Bopp, *Z. Naturforsch.* **40a**, 1235 (1985).
- [13] Gy. I. Szász and K. Heinzinger, *Earth Planet. Sci. Lett.* **64**, 163 (1983).
- [14] Gy. I. Szász, K. Heinzinger, and W. O. Riede, *Z. Naturforsch.* **36a**, 1067 (1981).
- [15] Y. Tamura, K. Tanaka, E. Spohr, and K. Heinzinger, *Z. Naturforsch.* **43a**, 1103 (1988).
- [16] M. F. Holovko and I. R. Yukhnovsky, in: *The Chemical Physics of Solvation, Part A* (R. R. Dogonadze, E. Kálman, A. A. Kornyshev, and J. Ulstrup, eds.), Elsevier, Amsterdam 1985.
- [17] M. F. Holovko, Yu. V. Kalyuzhny, and K. Heinzinger, *Ukrainian Academy of Sciences, Institute for Theoretical Physics (ITP)-Report Nr. 81 E*, Kiev 1987, 36 p.
- [18] F. H. Stillinger and A. Rahman, *J. Chem. Phys.* **60**, 1545 (1974).
- [19] P. Bopp, G. Jancsó, and K. Heinzinger, *Chem. Phys. Lett.* **98**, 129 (1983).
- [20] D. Chandler and H. C. Andersen, *J. Chem. Phys.* **57**, 1930 (1972).
- [21] J. D. Weeks, D. Chandler, and H. C. Andersen, *J. Chem. Phys.* **54**, 5237 (1971); **56**, 3812 (1972).
- [22] P. J. Rossky, *Pure Appl. Chem.* **57**, 1043 (1985).
- [23] G. Pálkás, P. Bopp, G. Jancsó, and K. Heinzinger, *Z. Naturforsch.* **39a**, 179 (1984).
- [24] A. G. Kalinichev, *Int. J. Thermophys.* **7**, 887 (1986).
- [25] D. C. Rapaport and H. A. Scheraga, *J. Phys. Chem.* **86**, 873 (1982).
- [26] Gy. I. Szász and K. Heinzinger, *Z. Naturforsch.* **38a**, 214 (1983).